Ion mobility–mass spectrometry with a radial opposed migration ion and aerosol classifier (ROMIAC)

May 15, 2013

W. Mui*, D. A. Thomas†, A. J. Downard†, J. L. Beauchamp†, J. H. Seinfeld*†, R. C. Flagan*†‡

Supporting Information

*Division of Engineering and Applied Science, California Institute of Technology, Pasadena, California 91125, USA

†Division of Chemistry and Chemical Engineering, California Institute of Technology, Pasadena, California 91125, USA

‡Corresponding author: flagan@caltech.edu

Introduction to FRIPS

Free radical initiated peptide sequencing (FRIPS) is an alternative method for the gas–phase sequencing that gives information complementary to that obtained by traditional CID or ECD/ETD experiments [1]. In this technique, a free radical precursor is attached to the N–terminus of a peptide or protein via standard NHS–activated coupling. When the derivatized peptide is subjected to collisional activation, loss of the free radical precursor via homolytic bond cleavage generates an acetyl radical at the N–terminus of the peptide. This radical then abstracts a hydrogen atom from various sites along the peptide, yielding side chain loss or cleavage of the C_α–C backbone bond through β–elimination. The product ions formed are highly sensitive to the C_β–H bond dissociation energy (BDE) of each amino acid residue, with residues possessing high C_β–H preferentially generating side chain loss and those with low C_β–H leading to backbone dissociation [2]. Figure S1 shows a general schematic of the current generation of FRIPS reagent, which utilizes the 2,5–dioxopyrrolidin–1–yl 2–(2,2,6,6–tetramethylpiperidin–1–yloxy)acetate (TEMPO–NHS) as the free radical precursor. Free radical product ions may also be generated in the MS^2 spectrum via reaction of generated acetyl radical without further collisional activation.

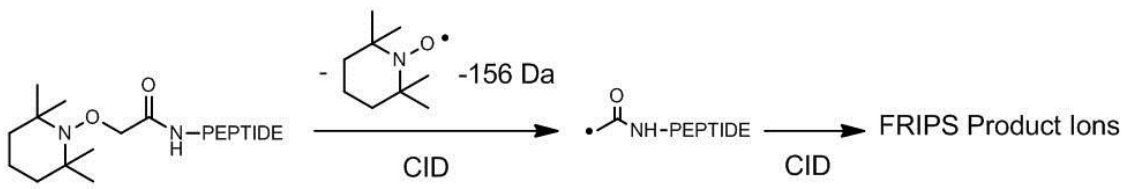

Supplementary Figure 1: Schematic of FRIPS methodology; the TEMPO precursor is coupled to the N-terminus of the peptide, and subsequent collisional activation leads to loss of the TEMPO moiety, generating an acetyl radical. CID of this radical then leads to hydrogen atom abstraction and followed by dissociation of the amino acid side chain or backbone.

Materials and Methods

Synthesis of TEMPO–based FRIPS Reagent

The TEMPO-based FRIPS reagent recently developed by Sohn and coworkers in the Beauchamp group, based upon the procedure outlined by Lee and coworkers [3], was synthesized and employed for free radical generation [4]. Briefly, the FRIPS reagent was synthesized from a methyl 2–bromoacetate starting compound, to which the TEMPO (2,2,6,6–Tetramethylpiperidine–1–oxyl) reagent was coupled to give methyl 2–(2,2,6,6–tetramethylpiperidin–1–yloxy)acetate. This compound was then converted to 2–(2,2,6,6–tetramethylpiperidin–1–yloxy)acetic acid by stirring in 2M KOH in THF for 24 h. The free acid was then activated by mixing with trifluoroacetic N–hydroxysuccinimide ester in dry DMF for 24 h to yield 2,5–dioxopyrrolidin–1–yl 2–(2,2,6,6–tetramethylpiperidin–1–yloxy)acetate, the desired TEMPO–based FRIPS reagent.

Model Peptide Derivatization

To derivatize the model peptides, ∼1 mg of a peptide was dissolved in 1 mL of a 50/50 (v/v) mixture of acetonitrile and water, vortexed for 3 min, sonicated for 15 min, and centrifuged at 4500 rpm for 5 min. A reaction mixture of 50 μL of peptide supernatant and 10 μL of a 10 μg/μL solution of FRIPS reagent in acetonitrile in a 100 mM triethylammonium bicarbonate buffer (pH 8.5) was prepared. The reaction was allowed to proceed for 2 hr and then quenched by addition of 2 μL of formic acid. The solvent was removed with use of a rotary evaporator, and the sample was resuspended in 10 μL of 0.1% trifluoroacetic acid and purified using a C18 ZipTip (Millipore, Billerica, MA) according to manufacturer protocol. The eluted sample was increased to a final volume of 500 μL in 49% methanol, 49% water, and 2% acetic acid (v/v).

Experimental Setup

The experimental setup consists of an electrospray ion source (ESI), the ROMIAC, and a Finnigan LTQ–MS (Thermo Electron Corp.); a detailed schematic is shown in Fig. S2. A syringe pump

fitted with a 250 μL syringe (Hamilton Co., GASTIGHT 1725) supplies solution at a rate of 5 $\mu\mathrm{L} \cdot \mathrm{min}^{-1}$ to the ESI, which is maintained at 5 kV potential relative to ground by a high voltage power supply (Acopian PO10HD6). Two equal flows of compressed N_2 gas are cleaned through a HEPA filter (Pall Life Sciences HEPA Capsule) and enter the ESI chamber perpendicular to the spray needle and convey ions to the ROMIAC. The ESI N_2 flow is measured by monitoring the pressure drop through a laminar flow element (LFE) using a differential pressure transducer; the ESI gas temperature, T_{ESI}, is heated for some experiments via heating tape wrapped around the two gas inlet tubes to the ESI chamber, controlled by a variable autotransformer (Variac Type W5MT3) and measured with a thermocouple (Omega 871 Digital Thermometer). All TAAX, UB, and model peptide measurements were performed at $T_{ESI} = 298$ K, while BK, AT1, and AT2 measurements were done at both $T_{ESI} = 298$ K and 400 K.

The cross–flow gas through the ROMIAC is also compressed N_2 that is cleaned through a HEPA filter and regulated with a proportioning solenoid valve (MKS Instruments Inc. 0248-20000SV). The cross–flow is exhausted through a vacuum pump (GAST 1023-101Q-G608X), with the flow rate kept constant by a critical orifice at the inlet to the vacuum pump. The flow rate of the classified ion flow leaving the ROMIAC is also monitored with a LFE. All experiments were run at $Q_x = 34.3$ lpm and $Q_s = 1.70$ lpm, resulting in $R_{nd} = 20.2$, and the cross–flow gas temperature, T_x, was 298 K. Analytes were at atmospheric pressure the entire journey from the ESI spray needle to the LTQ–MS inlet, the duration of which is estimated to be on the order of tens to hundreds of milliseconds.

A proportional–integral–differential (PID) algorithm written in LabView provided feedback control of the sample and classified flow based on signals from the differential pressure transducers that monitor the pressure drops across the LFEs. Since the exiting cross–flow is held constant via a critical orifice, the incoming and exiting cross–flows were matched by the proportioning solenoid valve until the sample and classified flows were balanced. The LabView program also controlled the high voltage supply (EMCO High Voltage CA12N) to select the target ion mobility. Ion mobility spectra were obtained by stepping through a range of voltages and monitoring the LTQ–MS signal.

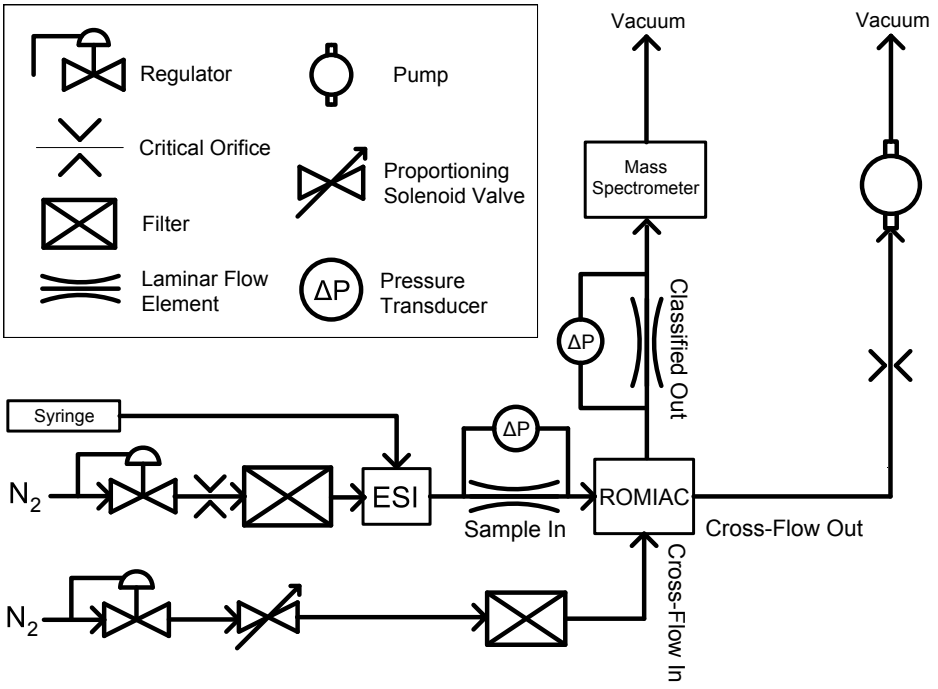

Supplementary Figure 2: Diagram of ESI–ROMIAC–LTQ–MS setup used to measure TAAX ion and peptide mobilities and cross sections. Flows were controlled both manually (with regulators and criticial orifices) and automatically (with P–I–D input to solenoid valves) via a custom LabView program that responded to measured gas flows through the laminar flow elements. The program also varied the voltage across the ROMIAC electrodes.

Supplementary Table 1: LTQ–MS settings.

Electrospray Voltage	5 kV
Sheath Gas Flow Rate	1.7 lpm
Cross Flow Rate	34.3 lpm
Capillary Voltage	0 V
Capillary Temp	50° C
Tube Lens Voltage	88 V
Multipole 00 Offset	-3.7 V
Lens 0 Voltage	-4.3 V
Multipole 0 Offset	-4.6 V
Gate Lens Voltage	-38.5 V
Multipole 1 Offset	-8.9 V
Multipole RF Amplitude	400 $V_{p\text{-}p}$
Front Lens	-4.9 V
Front Section	-8.8 V
Center Section	-11.9 V
Back Section	-6.75 V
Back Lens	0 V
Trap Eject Offset	0 V
q value	0.25
Activation Time	30 ms
% Collisional Activation	10%

Supplementary Table 2: m/z ranges used for mass–resolving ions.[a]

Species	m/z range	Species	m/z range
C2 monomer^{+1}	129–134	BK^{+1}	1059–1064
C2 dimer^{+1}	339–344	BK^{+2}	529–534
C2 trimer^{+1}	549–554	AT1^{+1}	1296–1301
C2 tetramer^{+1}	759–764	AT1^{+2}	647–652
C2 pentamer^{+1}	969–974	AT1^{+3}	431–436
C2 hexamer^{+1}	1180–1185	AT2^{+1}	1045–1050
C2 heptamer^{+1}	1390–1395	AT2^{+2}	522–527
C2 octamer^{+1}	1600–1605	UB^{+5}	1712–1717
C2 nonamer^{+1}	1810–1815	UB^{+6}	1426–1431
C3 monomer^{+1}	185–190	UB^{+7}	1222–1227
C3 dimer^{+1}	498–503	UB^{+8}	1069–1074
C3 trimer^{+1}	811–816	AARAAATAA b_3–NH_3 fragment	281.5
C3 tetramer^{+1}	1124–1129	AARAAATAA b_4–NH_3 fragment	352.5
C3 pentamer^{+1}	1437–1442	AARAAATAA b_5–NH_3 fragment	423.5
C3 hexamer^{+1}	1750–1755	AATAAARAA b_5–H_2O fragment	367.5
C4 monomer^{+1}	241–246	AATAAARAA b_6–H_2O fragment	438.5
C4 dimer^{+1}	563–568	AATAAARAA y_6 fragment	529.6
C4 trimer^{+1}	886–891	TEMPO–AARAAATAA a_6+H· fragment	526
C4 tetramer^{+1}	1208–1213	TEMPO–AARAAATAA c_6 fragment	570
C4 pentamer^{+1}	1530–1535	TEMPO–AATAAARAA y_6 fragment	530
C4 hexamer^{+1}	1853–1558	TEMPO–AATAAARAA z_7–H fragment	613
C5 monomer^{+1}	297–302	AARAAHAMA b_7–NH_3 fragment	631.5
C5 dimer^{+1}	676–681	AARAAMAHA b_7 fragment	642.5
C5 trimer^{+1}	1054–1059	TEMPO–AARAAHAMA a_6 fragment	591
C5 tetramer^{+1}	1432–1437	TEMPO–AARAAMAHA a_8 fragment	793.8
C5 pentamer^{+1}	1811–1816		
C6 monomer^{+1}	353–358		
C6 dimer^{+1}	788–793		
C6 trimer^{+1}	1222–1227		
C6 tetramer^{+1}	1657–1662		
C7 monomer^{+1}	409–414		
C7 dimer^{+1}	899–904		
C7 trimer^{+1}	1389–1394		
C7 tetramer^{+1}	1879–1884		
C8 monomer^{+1}	465–470		
C8 dimer^{+1}	1012–1017		
C8 trimer^{+1}	1559–1564		
C12 monomer^{+1}	690–695		
C12 dimer^{+1}	1461–1466		

[a]C2–C8 and C12 TAAX ions are brominated, except for C3 ions, which are iodinated. m/z ranges across 5 Da to include C isotopes.

Calibration Procedure

C2–C8 and C12 TAAX monomer ions were used as instrument calibration standards, as their reduced mobilities are unaffected by trace carrier gas contaminants and temperature [5, 6, 7]. TAAX monomer ion mobility values are from [6]. There is a linear relationship ($R^2 > 0.999$) between K_i^{-1} and ϕ_i^* of the TAAX monomer standards (Fig. S3). This relationship is used to determine K_i and reduced mobilities, $K_{0,i}$, of C2–C8 and C12 anion–coordinated multimer species (see SI). Ω_i of BK^{+1}, BK^{+2}, $AT2^{+1}$, $AT2^{+2}$, UB^{+7}, and UB^{+8} from [8, 9] were used for mobility calibration of the ROMIAC. A linear relationship exists between ϕ_i^* and K_i^{-1}, and K_i^{-1} is related to Ω_i via the Mason–Schamp equation [10]. For a mobility calibrant displaying multiple gas–phase conformers, the conformer making up the greatest proportion of the total signal in the classification spectrum was taken as the conformer corresponding to ϕ_i^* for the calibrant. The relationship between Ω_i and a coefficient β (a grouping of constants from the Mason–Schamp equation), is linear ($R^2 > 0.996$; Fig. S4). Each mobility spectrum was deconvoluted and peaks corresponding to a species were fitted to a Gaussian function. The contribution of each species to the total signal was estimated by calculating the integral under the Gaussian function.

Calculations

Reduced Mobility and Collisional Cross–Section

Calculated mobilities were converted to reduced mobilities, $K_{0,i}$, by the relationship

$$K_{0,i} = K_i \left(\frac{273.15 \text{ K}}{T} \right) \left(\frac{p}{101325 \text{ Pa}} \right) \tag{1}$$

where T is the carrier gas temperature and p is the carrier gas pressure.

Collisional cross–section values of BK^{+1}, BK^{+2}, $AT2^{+1}$, $AT2^{+2}$, UB^{+7}, and UB^{+8} from [8, 9] were used in the mobility calibration of the ROMIAC. There is a linear relationship between ϕ_i^* and

K_i^{-1}, and K_i^{-1} is related to Ω_i via the Mason–Schamp equation [10]:

$$K_i = \frac{3}{16}\frac{q_i}{N}\left(\frac{1}{m_i}+\frac{1}{M}\right)^{1/2}\left(\frac{2\pi}{kT}\right)^{1/2}\frac{1}{\Omega_i} \tag{2}$$

where $q_i = z_i e$ is the ionic charge, $N = \frac{p}{kT}$ is the carrier gas number density via the ideal gas law, k is the Boltzmann constant, m_i is the ion mass, and M is the carrier gas mass. Therefore, ϕ_i^* can be related to Ω_i via a coefficient, β:

$$\Omega_i \sim \beta K_i^{-1} \sim \beta\phi_i^* = \left(q_i\left(\frac{m_i+M}{m_i M}\right)^{1/2}T^{1/2}\right)\phi_i^* \tag{3}$$

In the case of a mobility calibrant displaying a multi–peaked signal, the peak making up the greatest proportion of the total signal was taken as the peak corresponding to ϕ_i^* for the calibrant. The relationship between Ω_i and β is linear ($R^2 > 0.996$), as shown in Fig. S4. It must be noted that there is a very large standard error of the intercept relative to the intercept value (see Fig. S4) due to a limited range of Ω covered by only nine mobility calibrant ions (i.e. non of the calibrant ions had a mobility near zero), which can result in large uncertainties when using the calibration to determine a Ω value for other biomolecules.

Signal Deconvolution and Fitting

Each classification signal, S, for TAAX ions, peptides, and model peptides was fitted to a Gaussian function of the form

$$S = \sum_{j=1}^{n} a_j e^{\left[-\left(\frac{\phi-b_j}{c_j}\right)^2\right]} \tag{4}$$

where a is the peak amplitude, b is the centroid, c is related to the peak width, and n is the number of peaks. The value $\Delta\phi_{FWHM}$ is then calculated as:

$$\Delta\phi_{FWHM,j} = 2\left(\ln\left(2\right)\right)^{1/2}c_j \tag{5}$$

A single peak was fitted to the signal if it appeared to be composed of one peak and the resulting value of R was no more than R_{nd}. If the signal appeared to be composed of multiple peaks, additional Gaussian terms were attempted to be fitted to where they were visually evident, with consideration that the values of R could not surpass R_{nd}.

In the case of multi–peaked signals, the proportion of each species' contribution to the total signal was estimated by calculating the integral under each Gaussian term, A_j,

$$A_j = a_j c_j \pi^{1/2} \tag{6}$$

and then calculating the fraction $\frac{A_j}{\sum_{j=1}^{n} A_j}$.

Results

Discussion of Effect of Field–Induced Heating

An ion's mobility, and therefore its cross section, is dependent on the ratio of the electric field, E, to the concentration of neutral particles, N [11]. Inside the classification region of the ROMIAC, the electric field is ∼100 V/cm, the pressure, p, is 101,325 Pa, and the temperature, T, is 298 K. Under these conditions, the E/N ratio is $\sim 3 \times 10^{-19}$ Townsends, which means that field–induced heating is negligible in this study.

In addition, note that N_2 molecule collisions in the ROMIAC orthogonal cross–flow classification region are unlikely to significantly increase the internal energy of analyte ions since the mean velocity of molecules in the cross–flow is only $\sim 10^{-1}$ m/s, much smaller than the background mean velocity of the bath molecules at 298 or 400 K ($\sim 10^1$ to 10^3 m/s).

Calibrations

Instrument and mobility calibrations show a linear response in $K_{0,i}$ to ϕ with TAAX ion standards ($R^2 > 0.999$; Fig. S3) and Ω_i to β with calibrant peptides ($R^2 > 0.996$; Fig. S4). The ROMIAC

also demonstrates high resolution with the TAAX standards (close to R_{nd}; Table S4), though resolution of the calibrant peptides and proteins were generally not as high as those of the TAAX standards (Table S6). This reduced resolution for peptides is fairly typical and is often assigned to the existence of multiple conformers within the mobility envelope [12, 13, 14, 15, 16, 17]. The instrument calibration linearity demonstrates that the ROMIAC provides accurate $K_{0,i}$ and Ω_i values for small ions unaffected by either ESI solvents (e.g. water and methanol) in the carrier gas or concave surfaces that increase the momentum transfer cross section, while the mobility calibration linearity suggests that drag factors and/or trace solvents affected the observed calibrant peptide Ω_i values in a similar fashion. Such solvents can complex with analyte ions [18, 5] and make complete desolvation of ions a challenge, thereby resulting in larger apparent Ω_i values. In addition, large peptides and proteins can present more surface area than a spherical particle of similar size, due to concavity and interior cavities, thereby increasing ion–buffer gas interactions and observed Ω_i values [19].

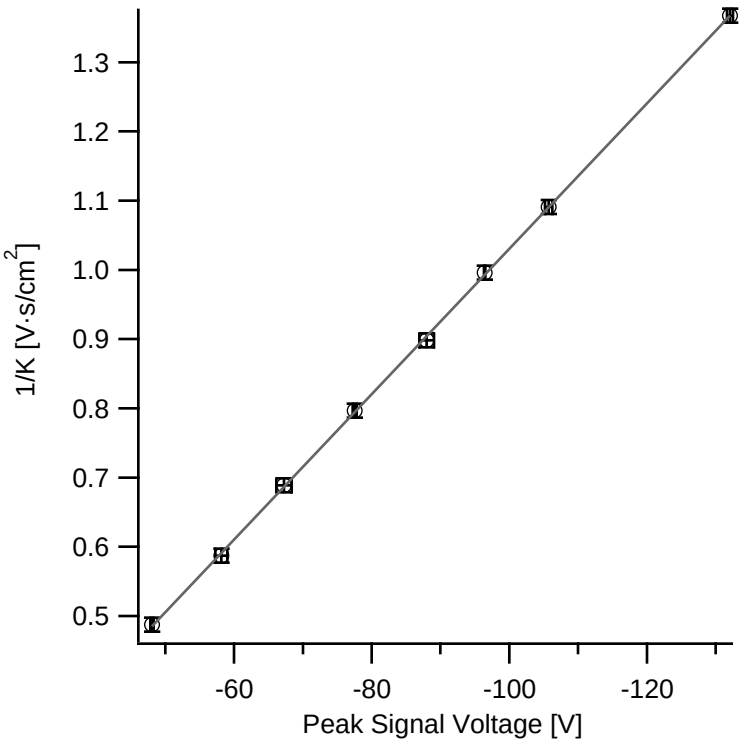

Supplementary Figure 3: ROMIAC instrument calibration with TAAX salts. Vertical error bars represent 1 standard deviation of K_i values from [6]. Horizontal error bars represent 1 standard deviation of ϕ_i^* for a TAAX ion. Fit is linear with $R^2 > 0.999$. Slope is $-0.0105 \pm (4.89 \times 10^{-5})$. Intercept is -0.0195 ± 0.00430.

Supplementary Table 3: Instrument calibration tetra–alkyl ammonium halide (TAAX) anion–coordinated singly–charged multimer Ω_i and $K_{0,i}$.[a]

TAAX	k Number of TAAX Units	Ω_i $\left[\text{Å}^2\right]$	$K_{0,i}$ $[\text{cm}^2\text{V}^{-1}\text{s}^{-1}]$
C2	2	225±2.7	0.94±0.011
C2	3	256±7.3	0.81±0.023
C2	4	251±3.2	0.82±0.010
C2	5	298±2.7	0.69±0.006
C2	6	325±3.3	0.63±0.007
C2	7	353±4.0	0.58±0.007
C2	8	377±3.4	0.54±0.005
C2	9	405±4.3	0.50±0.005
C3	2	222±3.1	0.94±0.013
C3	3	289±5.8	0.71±0.014
C3	4	333±8.0	0.62±0.015
C3	5	369±4.0	0.56±0.006
C3	6	430±4.1	0.48±0.005
C4	2	250±2.7	0.83±0.009
C4	3	321±3.6	0.64±0.007
C4	4	353±4.8	0.58±0.008
C4	5	399±6.6	0.51±0.008
C4	6	461±5.3	0.44±0.005
C5	2	282±2.5	0.73±0.007
C5	3	354±3.2	0.58±0.005
C5	4	409±4.7	0.50±0.006
C5	5	440±6.1	0.46±0.006
C6	2	310±3.0	0.67±0.006
C6	3	386±3.5	0.53±0.005
C6	4	449±3.8	0.46±0.004
C7	2	335±2.8	0.61±0.005
C7	3	419±3.0	0.49±0.004
C7	4	491±3.7	0.42±0.003
C8	2	361±2.9	0.57±0.005
C8	3	454±3.4	0.45±0.003
C12	2	445±3.7	0.46±0.004

[a]In N_2 at atmospheric pressure and $T_{ESI} = T_x = 298$ K. Values are the average of three scans. Note that C3 species are iodinated while all other TAAX species are brominated. Detailed signal, Gaussian fit, and resolution values are found in Table S4.

Supplementary Table 4: TAAX instrument calibration detailed results.[a]

TAAX	Trial	[b]$K_{0,i}$	Start ϕ [-V]	End ϕ [-V]	a_j	a_j 95% CI	b_j	b_j 95% CI	c_j	c_j 95% CI	FWHM [V]	E (FWHM) [V]	R	E (R)	$\overline{\phi_i^*}$ [V]	$\sigma_{\overline{\phi_i^*}}$ [V]	$\overline{K_i}$	$\overline{K_i^{-1}}$
C2	1	1.88	40	60	1.043	0.033	-48.29	0.03	1.399	0.051	2.3303	0.0852	20.72	0.77	-48.06	0.23	2.052	0.487
C2	2	1.88	40	60	1.024	0.084	-48.08	0.10	1.634	0.155	2.7222	0.2583	17.66	1.71				
C2	3	1.88	40	60	1.040	0.039	-47.82	0.05	1.632	0.071	2.7176	0.1191	17.59	0.79				
C3	1	1.56	45	205	0.966	0.026	-57.84	0.04	1.986	0.062	3.3068	0.104	17.49	0.56	-58.16	0.86	1.702	0.587
C3	2	1.56	45	205	1.006	0.027	-57.51	0.05	2.203	0.070	3.6689	0.1176	15.67	0.51				
C3	3	1.56	45	205	0.957	0.036	-59.14	0.05	1.818	0.079	3.0271	0.1319	19.53	0.86				
C4	1	1.33	60	240	1.029	0.029	-66.22	0.06	2.742	0.089	4.566	0.1491	14.50	0.48	-67.26	1.09	1.451	0.688
C4	2	1.33	60	240	1.017	0.022	-67.15	0.04	2.421	0.062	4.0327	0.1035	16.65	0.43				
C4	3	1.33	60	240	1.023	0.027	-68.41	0.04	2.215	0.068	3.6883	0.1145	18.54	0.58				
C5	1	1.15	60	240	1.025	0.014	-77.90	0.02	2.619	0.041	4.3617	0.0696	17.86	0.29	-77.54	0.31	1.255	0.796
C5	2	1.15	60	240	1.032	0.016	-77.40	0.03	2.679	0.050	4.4612	0.0832	17.35	0.33				
C5	3	1.15	60	240	1.039	0.016	-77.32	0.03	2.712	0.050	4.517	0.0842	17.11	0.32				
C6	1	1.02	75	225	1.050	0.097	-86.88	0.12	1.629	0.173	2.7131	0.2896	32.02	3.46	-87.98	1.08	1.113	0.898
C6	2	1.02	75	225	1.015	0.113	-87.21	0.34	3.750	0.483	6.2457	0.805	13.96	1.85				
C6	3	1.02	75	225	0.861	0.144	-88.75	0.40	2.918	0.566	4.8593	0.943	18.26	3.62				
C7	1	0.92	85	235	1.036	0.010	-96.43	0.02	3.326	0.040	5.5381	0.0671	17.41	0.21	-96.41	0.08	1.004	0.995
C7	2	0.92	85	235	1.028	0.010	-96.31	0.02	3.305	0.037	5.5031	0.0628	17.50	0.20				
C7	3	0.92	85	235	1.007	0.012	-96.48	0.03	3.284	0.046	5.4696	0.0781	17.64	0.25				
C8	1	0.84	90	240	1.041	0.009	-105.48	0.02	3.775	0.041	6.2871	0.0684	16.77	0.18	-105.73	0.54	0.916	1.090
C8	2	0.84	90	240	1.036	0.007	-105.36	0.02	3.736	0.030	6.2213	0.051	16.93	0.14				
C8	3	0.84	90	240	1.030	0.007	-106.36	0.02	3.625	0.028	6.0362	0.0473	17.62	0.14				
C12	1	0.67	120	220	1.013	0.013	-132.53	0.04	4.359	0.065	7.2593	0.1089	18.25	0.28	-132.08	0.42	0.731	1.367
C12	2	0.67	120	220	1.012	0.015	-131.70	0.06	4.782	0.085	7.9633	0.1418	16.53	0.30				
C12	3	0.67	120	220	1.033	0.015	-132.02	0.05	4.351	0.077	7.2464	0.1286	18.21	0.33				

[a]C2–C8 and C12 TAAX ions are brominated, except for C3 ions, which are iodinated. $T_x = T_{ESI} = 298$ K.
[b]Values from [6]. Mobility values are in units of $[\mathrm{cm}^2 \cdot \mathrm{V}^{-1} \cdot \mathrm{s}^{-1}]$.

Supplementary Table 5: TAAX salt ions detailed results.

Species	Trial	k-mer	Start ϕ [V]	End ϕ [V]	a	a 95%CI	b	b 95%CI	c	c 95%CI	FWHM	E(FWHM)	R	E(R)	avg c [V]	σ(avg c)	$1/K$ [V-s/cm^2]	E($1/K$)	$1/K$ rel. err.	K [cm^2/V/s]	E(K)	m/z	Ion Mass [kg]	Ω [Å^2]	E(Ω)	K_o [cm^2/V/s]	E(K_o)
T12AB	1	2	120	220	1.02	0.02	-192.22	0.09	5.51	0.12	9.18	0.20	20.94	0.47	-192.00	0.26	2.00	0.02	0.008	0.50	0.004	771.22	2.43E-24	445	3.7	0.46	0.004
T12AB	2	2	120	220	1.00	0.02	-191.72	0.08	5.49	0.11	9.14	0.18	20.97	0.42													
T12AB	3	2	120	220	1.00	0.02	-192.05	0.07	5.47	0.11	9.11	0.18	21.09	0.42													
T7AB	1	2	85	235	1.03	0.02	-144.08	0.05	4.07	0.08	6.78	0.13	21.26	0.40	-144.11	0.10	1.49	0.01	0.008	0.67	0.006	490.69	1.50E-24	335	2.8	0.61	0.005
T7AB	2	2	85	235	1.02	0.02	-144.02	0.05	4.02	0.07	6.70	0.12	21.51	0.38													
T7AB	3	2	85	235	1.03	0.02	-144.22	0.05	4.02	0.07	6.70	0.12	21.53	0.38													
T7AB	1	3	85	235	0.95	0.01	-180.47	0.06	5.13	0.09	8.55	0.15	21.12	0.37	-180.43	0.04	1.87	0.01	0.007	0.53	0.004	490.69	2.31E-24	419	3.0	0.49	0.004
T7AB	2	3	85	235	0.98	0.01	-180.39	0.06	5.16	0.08	8.59	0.14	20.99	0.34													
T7AB	3	3	85	235	1.00	0.01	-180.42	0.06	5.25	0.08	8.74	0.13	20.64	0.32													
T7AB	1	4	85	235	0.94	0.05	-211.52	0.31	7.78	0.44	12.96	0.73	16.32	0.94	-211.75	0.20	2.20	0.02	0.008	0.45	0.003	490.69	3.13E-24	491	3.7	0.42	0.003
T7AB	2	4	85	235	0.84	0.04	-211.91	0.22	5.85	0.31	9.74	0.51	21.77	1.16													
T7AB	3	4	85	235	0.96	0.05	-211.81	0.28	6.39	0.40	10.63	0.66	19.92	1.27													
T3AI	1	2	45	205	0.85	0.07	-94.65	0.24	3.61	0.34	6.01	0.57	15.75	1.54	-94.80	0.44	0.98	0.01	0.014	1.02	0.014	313.26	8.29E-25	222	3.1	0.94	0.013
T3AI	2	2	45	205	0.87	0.06	-94.45	0.19	3.49	0.26	5.81	0.44	16.25	1.26													
T3AI	3	2	45	205	0.84	0.06	-95.30	0.18	2.90	0.25	4.83	0.41	19.74	1.72													
T3AI	1	3	45	205	0.69	0.09	-124.84	0.89	8.82	1.26	14.69	2.10	8.50	1.28	-124.44	1.48	1.29	0.03	0.020	0.78	0.016	313.26	1.35E-24	289	5.8	0.71	0.014
T3AI	2	3	45	205	0.81	0.09	-122.80	0.63	6.91	0.89	11.50	1.49	10.68	1.43													
T3AI	3	3	45	205	0.67	0.07	-125.67	0.95	10.51	1.35	17.50	2.24	7.18	0.97													
T3AI	1	4	45	205	0.56	0.06	-146.37	1.30	14.67	1.83	24.43	3.05	5.99	0.80	-143.71	2.31	1.49	0.04	0.024	0.67	0.016	313.26	1.87E-24	333	8.0	0.62	0.015
T3AI	2	4	45	205	0.60	0.08	-142.58	1.51	13.43	2.13	22.36	3.55	6.38	1.08													
T3AI	3	4	45	205	0.50	0.06	-142.18	1.41	13.77	1.99	22.93	3.31	6.20	0.96													
T3AI	1	5	45	205	0.91	0.04	-159.13	0.16	4.34	0.23	7.22	0.39	22.04	1.21	-159.16	0.57	1.65	0.02	0.011	0.61	0.007	313.26	2.39E-24	369	4.0	0.56	0.006
T3AI	2	5	45	205	0.81	0.04	-158.61	0.22	5.39	0.31	8.97	0.52	17.67	1.04													
T3AI	3	5	45	205	0.86	0.04	-159.74	0.19	5.38	0.27	8.97	0.45	17.82	0.91													
T3AI	1	6	45	205	0.75	0.10	-186.06	0.43	3.75	0.60	6.24	1.00	29.83	4.87	-185.55	0.50	1.93	0.02	0.010	0.52	0.005	313.26	2.91E-24	430	4.1	0.48	0.005
T3AI	2	6	45	205	0.82	0.07	-185.53	0.44	6.64	0.63	11.06	1.05	16.77	1.63													
T3AI	3	6	45	205	0.77	0.07	-185.06	0.32	4.28	0.45	7.13	0.74	25.97	2.76													
T2AB	1	2	60	210	0.79	0.11	-94.83	0.42	3.72	0.59	6.19	0.99	15.31	2.50	-95.10	0.26	0.98	0.01	0.012	1.02	0.012	210.16	5.65E-25	225	2.7	0.94	0.011
T2AB	2	2	60	210	0.96	0.13	-95.11	0.46	4.11	0.66	6.85	1.11	13.88	2.31													
T2AB	3	2	60	210	1.05	0.10	-95.34	0.24	2.95	0.34	4.92	0.56	19.39	2.26													
T2AB	1	3	60	210	0.84	0.13	-107.97	0.49	3.74	0.69	6.22	1.14	17.35	3.26	-109.38	2.16	1.13	0.03	0.029	0.89	0.025	210.16	9.14E-25	256	7.3	0.81	0.023
T2AB	2	3	60	210	0.43	0.08	-108.30	2.37	16.11	3.35	26.82	5.59	4.04	0.93													
T2AB	3	3	60	210	0.62	0.07	-111.86	1.67	17.17	2.37	28.59	3.94	3.91	0.60													
T2AB	1	4	60	210	0.81	0.05	-107.75	0.20	4.18	0.28	6.96	0.46	15.47	1.06	-107.97	0.44	1.11	0.01	0.013	0.90	0.011	210.16	1.26E-24	251	3.2	0.82	0.010
T2AB	2	4	60	210	0.86	0.05	-107.69	0.19	3.74	0.26	6.23	0.44	17.28	1.25													
T2AB	3	4	60	210	0.82	0.05	-108.48	0.18	3.90	0.26	6.49	0.43	16.72	1.14													
T2AB	1	5	60	210	0.93	0.03	-128.56	0.08	3.40	0.11	5.67	0.18	22.68	0.75	-128.44	0.15	1.33	0.01	0.009	0.75	0.007	210.16	1.61E-24	298	2.7	0.69	0.006
T2AB	2	5	60	210	0.97	0.03	-128.27	0.08	3.67	0.12	6.11	0.19	21.00	0.68													
T2AB	3	5	60	210	0.97	0.02	-128.48	0.07	3.14	0.09	5.24	0.15	24.54	0.73													
T2AB	1	6	60	210	0.94	0.03	-140.36	0.09	4.00	0.13	6.66	0.22	21.07	0.72	-140.20	0.36	1.45	0.01	0.010	0.69	0.007	210.16	1.96E-24	325	3.3	0.63	0.007
T2AB	2	6	60	210	0.99	0.03	-139.78	0.09	3.83	0.13	6.37	0.21	21.93	0.75													
T2AB	3	6	60	210	0.91	0.04	-140.45	0.16	4.33	0.23	7.22	0.38	19.46	1.04													
T2AB	1	7	60	210	0.93	0.06	-151.95	0.27	5.26	0.39	8.75	0.64	17.36	1.31	-152.32	0.60	1.58	0.02	0.011	0.63	0.007	210.16	2.31E-24	353	4.0	0.58	0.007
T2AB	2	7	60	210	0.81	0.05	-152.01	0.26	5.12	0.36	8.53	0.60	17.82	1.29													
T2AB	3	7	60	210	0.81	0.05	-153.01	0.23	4.71	0.32	7.85	0.53	19.50	1.35													
T2AB	1	8	60	210	0.84	0.07	-163.16	0.30	4.57	0.42	7.61	0.70	21.43	2.01	-163.12	0.28	1.69	0.02	0.009	0.59	0.005	210.16	2.66E-24	377	3.4	0.54	0.005
T2AB	2	8	60	210	0.97	0.05	-163.37	0.21	4.83	0.29	8.05	0.49	20.30	1.25													
T2AB	3	8	60	210	0.90	0.06	-162.82	0.28	5.04	0.39	8.40	0.65	19.38	1.54													
T2AB	1	9	60	210	0.93	0.09	-174.19	0.31	3.92	0.44	6.52	0.73	26.72	3.04	-174.87	0.59	1.82	0.02	0.011	0.55	0.006	210.16	3.01E-24	405	4.3	0.50	0.005
T2AB	2	9	60	210	0.87	0.10	-175.31	0.60	6.73	0.85	11.21	1.42	15.64	2.04													
T2AB	3	9	60	210	0.81	0.11	-175.11	0.69	6.43	0.99	10.70	1.65	16.36	2.59													
T4AB	1	2	60	240	1.00	0.01	-106.80	0.02	3.06	0.03	5.10	0.05	20.95	0.21	-106.90	0.21	1.10	0.01	0.011	0.91	0.010	322.37	9.38E-25	250	2.7	0.83	0.009
T4AB	2	2	60	240	0.99	0.01	-106.76	0.02	3.05	0.03	5.08	0.05	21.03	0.22													
T4AB	3	2	60	240	1.01	0.01	-107.14	0.02	3.01	0.03	5.00	0.05	21.41	0.21													
T4AB	1	3	60	240	0.85	0.03	-138.05	0.11	3.93	0.16	6.55	0.26	21.08	0.85	-138.06	0.49	1.43	0.02	0.011	0.70	0.008	322.37	1.47E-24	321	3.6	0.64	0.007
T4AB	2	3	60	240	0.92	0.03	-137.58	0.09	3.90	0.13	6.49	0.21	21.20	0.71													
T4AB	3	3	60	240	1.01	0.03	-138.55	0.09	4.25	0.13	7.08	0.21	19.58	0.60													
T4AB	1	4	60	240	0.68	0.07	-152.09	0.91	11.34	1.28	18.88	2.13	8.05	0.96	-152.43	0.93	1.58	0.02	0.014	0.63	0.009	322.37	2.01E-24	353	4.8	0.58	0.008
T4AB	2	4	60	240	0.52	0.06	-151.71	0.99	11.28	1.41	18.79	2.34	8.07	1.06													
T4AB	3	4	60	240	0.55	0.06	-153.48	0.79	9.51	1.11	15.83	1.85	9.69	1.18													
T4AB	1	5	60	240	0.96	0.04	-172.75	0.20	5.52	0.29	9.20	0.48	18.79	1.00	-172.05	1.60	1.79	0.03	0.017	0.56	0.009	322.37	2.54E-24	399	6.6	0.51	0.008
T4AB	2	5	60	240	0.77	0.04	-170.21	0.42	9.43	0.59	15.70	0.99	10.84	0.71													
T4AB	3	5	60	240	0.87	0.05	-173.18	0.32	6.34	0.45	10.56	0.75	16.40	1.19													
T4AB	1	6	60	240	0.80	0.10	-200.08	0.56	5.35	0.79	8.91	1.31	22.45	3.36	-199.01	0.95	2.07	0.02	0.012	0.48	0.006	322.37	3.08E-24	461	5.3	0.44	0.005
T4AB	2	6	60	240	0.86	0.09	-198.69	0.59	6.67	0.84	11.10	1.40	17.90	2.30													
T4AB	3	6	60	240	0.73	0.09	-198.27	0.64	6.48	0.90	10.78	1.51	18.39	2.63													
T8AB	1	2	90	240	1.02	0.01	-155.25	0.04	4.44	0.06	7.39	0.10	21.00	0.28	-155.24	0.09	1.61	0.01	0.008	0.62	0.005	546.79	1.68E-24	361	2.9	0.57	0.005
T8AB	2	2	90	240	1.01	0.01	-155.15	0.04	4.43	0.06	7.38	0.10	21.02	0.29													
T8AB	3	2	90	240	1.05	0.02	-155.33	0.06	4.64	0.08	7.73	0.13	20.09	0.35													
T8AB	1	3	90	240	1.02	0.01	-195.50	0.06	5.26	0.08	8.77	0.13	22.31	0.35	-195.59	0.12	2.03	0.02	0.007	0.49	0.004	546.79	2.59E-24	454	3.4	0.45	0.003
T8AB	2	3	90	240	0.98	0.01	-195.54	0.06	5.15	0.08	8.58	0.14	22.80	0.37													
T8AB	3	3	90	240	1.01	0.01	-195.73	0.05	4.94	0.07	8.22	0.12	23.80	0.36													
T5AB	1	2	60	240	1.02	0.01	-121.00	0.02	3.59	0.03	5.98	0.05	20.23	0.19	-120.92	0.08	1.25	0.01	0.009	0.80	0.007	378.47	1.12E-24	282	2.5	0.73	0.007
T5AB	2	2	60	240	0.99	0.01	-120.84	0.03	3.60	0.04	6.00	0.07	20.14	0.23													
T5AB	3	2	60	240	0.99	0.01	-120.91	0.03	3.53	0.04	5.88	0.06	20.57	0.22													
T5AB	1	3	60	240	0.93	0.02	-152.30	0.06	3.81	0.08	6.35	0.13	23.98	0.50	-152.29	0.24	1.58	0.01	0.009	0.63	0.006	378.47	1.75E-24	354	3.2	0.58	0.005
T5AB	2	3	60	240	0.99	0.01	-152.05	0.05	4.30	0.07	7.15	0.11	21.26	0.34													
T5AB	3	3	60	240	0.79	0.03	-152.53	0.11	4.28	0.16	7.12	0.27	21.42	0.82													
T5AB	1	4	60	240	0.79	0.07	-175.80	0.30	4.26	0.42	7.10	0.70	24.76	2.48	-176.24	0.77	1.83	0.02	0.011	0.55	0.006	378.47	2.38E-24	409	4.7	0.50	0.006
T5AB	2	4	60	240	0.56	0.06	-175.78	0.83	8.85	1.17	14.74	1.95	11.93	1.63													
T5AB	3	4	60	240	0.71	0.07	-177.13	0.36	4.75	0.51	7.91	0.86	22.39	2.47													
T5AB	1	5	60	240	0.69	0.05	-191.19	0.62	9.63	0.88	16.04	1.46	11.92	1.13	-190.12	1.32	1.98	0.03	0.014	0.51	0.007	378.47	3.01E-24	440	6.1	0.46	0.006
T5AB	2	5	60	240	0.69	0.05	-190.52	0.66	10.12	0.93	16.86	1.54	11.30	1.07													
T5AB	3	5	60	240	0.46	0.04	-188.64	1.02	13.35	1.45	22.23	2.41	8.49	0.96													
T6AB	1	2	75	225	0.92	0.04	-133.20	0.14	3.85	0.20	6.40	0.33	20.80	1.08	-133.11	0.24	1.38	0.01	0.010	0.73	0.007	434.58	1.31E-24	310	3.0	0.67	0.006
T6AB	2	2	75	225	0.87	0.03	-132.84	0.10	3.64	0.14	6.06	0.24	21.90	0.89													
T6AB	3	2	75	225	0.93	0.04	-133.30	0.12	3.95	0.17	6.57	0.29	20.28	0.91													
T6AB	1	3	75	225	0.96	0.03	-166.65	0.11	4.28	0.16	7.13	0.26	23.36	0.86	-166.33	0.30	1.73	0.02	0.009	0.58	0.005	434.58	2.03E-24	386	3.5	0.53	0.005
T6AB	2	3	75	225	0.91	0.02	-166.27	0.08	4.39	0.11	7.31	0.18	22.74	0.58													
T6AB	3	3	75	225	0.96	0.02	-166.06	0.07	4.36	0.10	7.26	0.17	22.87	0.56													
T6AB	1	4	75	225	0.81	0.06	-194.10	0.17	2.71	0.24	4.52	0.40	42.98	3.88	-193.75	0.31	2.01	0.02	0.008	0.50	0.004	434.58	2.75E-24	449	3.8	0.46	0.004
T6AB	2	4	75	225	0.86	0.04	-193.49	0.17	4.58	0.24	7.62	0.39	25.38	1.33													
T6AB	3	4	75	225	0.80	0.06	-193.68	0.41	6.52	0.59	10.86	0.98	17.83	1.64													

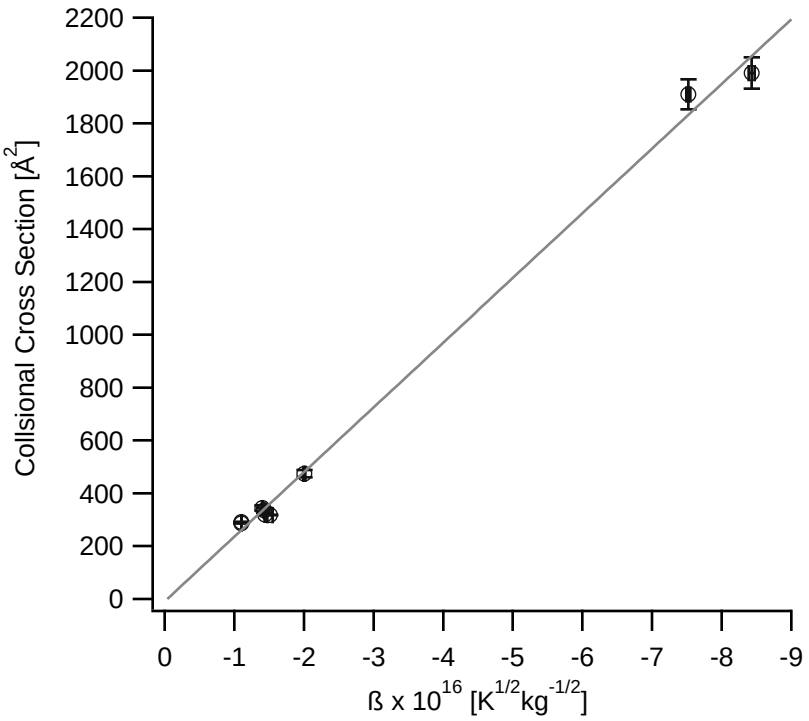

Supplementary Figure 4: ROMIAC mobility calibration with peptides. Vertical error bars represent 3% error in Ω_i values from [8]. Horizontal error bars represent 1 standard deviation of ϕ_i^* for a peptide ion. Fit is linear with $R^2 > 0.996$. Slope is $-244.779 \pm (5.573)$. Intercept is -9.145 ± 22.171.

Supplementary Table 6: Peptide mobility calibration detailed results.[a]

Peptide	Trial	+Charge	Start ϕ [-V]	End ϕ [-V]	a_j	a_j 95% CI	b_j	b_j 95% CI	c_j	c_j 95% CI	FWHM [V]	E (FWHM) [V]	R	E (R)	$\overline{\phi_i^*}$ [V]	$\sigma_{\overline{\phi_i^*}}$ [V]	Ω [Å^2]	E (Ω) [Å^2]	β	E (β)
BK	1	1	75	175	1.00	0.02	-135.67	0.11	4.06	0.09	6.75	0.15	20.09	0.46	-135.69	0.20	[c]292		-1.101	0.002
BK	2	1	75	175	0.99	0.01	-135.89	0.08	4.27	0.08	7.11	0.14	19.10	0.38						
BK	3	1	75	175	0.97	0.02	-135.50	0.09	4.02	0.08	6.69	0.13	20.26	0.42						
BK	1	2	75	175	0.66	0.58	-89.19	0.83	5.97	1.32	9.94	2.20	8.97	2.07	-88.73	0.41	[c]319		-1.439	0.007
BK	2	2	75	175	0.47	0.11	-88.45	0.24	3.62	0.63	6.03	1.04	14.66	2.57						
BK	3	2	75	175	0.61	0.26	-88.55	0.35	5.08	0.81	8.47	1.35	10.46	1.70						
AT2	1	1	75	180	0.98	0.01	-135.72	0.04	4.18	0.06	6.96	0.11	19.51	0.31	-135.76	0.15	[c]286		-1.101	0.001
AT2	2	1	75	180	1.01	0.01	-135.64	0.04	4.36	0.06	7.25	0.10	18.70	0.27						
AT2	3	1	75	180	1.01	0.01	-135.93	0.04	4.19	0.06	6.98	0.10	19.48	0.28						
AT2	1	2	75	180	0.72	0.42	-91.71	0.98	5.67	1.56	9.45	2.60	9.71	2.78	-93.36	2.32	[c]318		-1.515	0.038
BK	1	2	75	110	0.93	0.06	-86.77	0.21	4.05	0.21	6.74	0.34	12.87	0.69	-86.53	0.21	[d]344	10.32	-1.404	0.003
BK	2	2	75	110	0.91	0.05	-86.45	0.16	3.81	0.17	6.35	0.28	13.62	0.64						
BK	3	2	75	110	0.85	0.07	-86.37	0.20	3.98	0.21	6.63	0.35	13.02	0.71						
UB	1	7	80	160	0.93	0.04	-134.49	0.19	5.70	0.27	9.48	0.44	14.18	0.68	-133.94	0.52	[d]1910	57.3	-7.518	0.029
UB	2	7	80	160	0.96	0.03	-133.88	0.12	5.41	0.17	9.01	0.29	14.85	0.49						
UB	3	7	80	160	0.96	0.04	-133.46	0.17	5.14	0.25	8.56	0.41	15.60	0.77						
UB	1	8	80	160	0.85	0.04	-132.18	0.15	4.29	0.21	7.15	0.36	18.50	0.94	-131.43	0.68	[d]1990	59.7	-8.431	0.043
UB	2	8	80	160	1.01	0.05	-130.88	0.18	4.30	0.25	7.16	0.41	18.27	1.08						
UB	3	8	80	160	0.76	0.06	-131.22	0.32	5.17	0.45	8.62	0.75	15.23	1.36						
AT1	1	3	75	115	0.83	0.05	-83.33	0.19	4.32	0.27	7.20	0.46	11.57	0.76	-82.65	0.61	[d]474	14.22	-2.006	0.015
AT1	2	3	75	95	0.72	0.07	-82.43	0.41	5.30	0.61	8.83	1.01	9.34	1.11						
AT1	3	3	75	95	0.79	0.07	-82.17	0.32	4.25	0.46	7.07	0.77	11.62	1.31						
AT2	1	2	80	120	0.66	0.18	-88.17	0.19	3.31	0.51	5.51	0.85	16.00	2.51	-88.02	0.24	[d]335	10.05	-1.428	0.004
AT2	2	2	80	120	0.73	0.20	-88.16	0.16	3.39	0.45	5.65	0.74	15.61	2.08						
AT2	3	2	80	120	0.75	0.15	-87.74	0.14	3.55	0.36	5.91	0.60	14.85	1.53						

[a]C2–C8 and C12 TAAX ions are brominated, except for C3 ions, which are iodinated. $T_x = T_{ESI} = 298$ K.
[b]Values from [6]. Mobility values are in units of $[\mathrm{cm}^2 \cdot \mathrm{V}^{-1} \cdot \mathrm{s}^{-1}]$.
[c]Values from [9].
[d]Values from [8].

Supplementary Table 7: Mobility calibration bradykinin (BK), angiotensin I (AT1), angiotension II (AT2), and bovine ubiquitin (UB) Ω_i at T_{ESI} = 298 K, and comparison to literature values.[a]

Peptide	Peak #	Ω_i $\left[\text{Å}^2\right]$	[b]%Δ	[c]%Δ	[d]%Δ
BK^{+1}	1	172±29.3	-40.9%		
BK^{+1}	2	207±32.5	-29.0%		
$^{*}BK^{+1}$	3	261±29.5	-10.6%		
$^{*\#}BK^{+2}$	9	334±30.8	4.8%		-2.8%
BK^{+2}	10	365±32.7	14.5%		6.2%
$^{*}AT1^{+1}$	13	292±30.0			
$^{*}AT1^{+2}$	18	365±34.8		-5.0%	
$AT1^{+2}$	19	380±34.3		-1.2%	
$^{*\#}AT1^{+3}$	24	482±37.0		1.9%	1.7%
$^{*}AT2^{+1}$	26	258±28.5	-9.8%		
$AT2^{+1}$	27	278±29.3	-2.8%		
$^{*\#}AT2^{+2}$	32	340±31.1	7.0%	-4.1%	1.6%
$AT2^{+2}$	33	362±31.8	13.8%	1.9%	8.0%
$^{*}UB^{+5}$	36	1390±57.3			
$^{*}UB^{+6}$	37	1613±65.3			
$^{*\#}UB^{+7}$	38	1831±71.2			-4.1%
$^{*\#}UB^{+8}$	39	2055±79.8			3.2%

[a]In N_2 at atmospheric pressure, $T_{ESI} = T_x$ = 298 K. Values are the average of three scans. Peak numbers correspond to those labeled in Fig. 3 and Fig. S5. Detailed signal, Gaussian fit, proportion, and resolution values are found in Table S9.

*Indicates parent/dominant conformation for that species.

#Indicates peak was also used as a mobility calibrant.

References: [b][9] [c][20] [d][8].

Supplementary Table 8: Mobility calibration bradykinin (BK), angiotensin I (AT1), and angiotension II (AT2) Ω_i at $T_{ESI} = 400$ K, and comparison to literature values.[a]

Peptide	Peak #	Ω_i $\left[\text{Å}^2\right]$	[b]%Δ	[c]%Δ	[d]%Δ
BK^{+1}	4	216±25.3	-26.0%		
$^{*\#}BK^{+1}$	5	260±27.9	-10.9%		
BK^{+1}	6	277±28.0	-5.2%		
BK^{+1}	7	294±28.3	0.7%		
BK^{+1}	8	319±26.1	9.2%		
$^{*\#}BK^{+2}$	11	343±28.6	7.6%		-0.2%
BK^{+2}	12	370±29.1	15.8%		7.4%
$AT1^{+1}$	14	243±20.3			
$^{*}AT1^{+1}$	15	294±28.8			
$AT1^{+1}$	16	326±28.8			
$AT1^{+1}$	17	348±29.6			
$^{*}AT1^{+2}$	20	369±30.5		-4.0%	
$AT1^{+2}$	21	392±28.3		2.1%	
$AT1^{+2}$	22	424±20.1		10.4%	
$AT1^{+2}$	23	465±23.3		21.1%	
$^{*}AT1^{+3}$	25	510±31.7		7.9%	7.7%
$AT2^{+1}$	28	221±25.9	-22.7%		
$^{*\#}AT2^{+1}$	29	260±28.0	-8.9%		
$AT2^{+1}$	30	289±28.6	1.0%		
$AT2^{+1}$	31	309±28.6	7.9%		
$^{*\#}AT2^{+2}$	34	362±21.4	13.7%	1.9%	7.9%
$AT2^{+2}$	35	396±26.4	24.6%	11.6%	18.3%

[a]In N_2 at atmospheric pressure, $T_{ESI} = 400$ K and $T_x = 298$ K. Values are the average of three scans. Peak numbers correspond to those labeled in Fig. 3. Detailed signal, Gaussian fit, proportion, and resolution values are found in Table S10.

*Indicates parent/dominant conformation for that species.

#Indicates peak was also used as a mobility calibrant.

References: [b][9] [c][20] [d][8].

Supplementary Table 9: Peptides: detailed results at $T_{ESI} = 298$ K.

Species	Trial	Charge	Peak	Start Φ [V]	End Φ [V]	σ	σ 95%CI	b	b 95%CI	c	c 95%CI	FWHM	E(FWHM)	R	E(R)	A	avg 4	E(A)	Fraction	E(Fraction)	avg c [V]	σ(avg c)	Ion Mass [kg]	Red Mass [kg]	Θ·10^{44}	E(Θ)x10^{44}	Ω [Å^2]	E(Ω)	Hill1999	Raether2009	Robinson2010	%diff Hill	% diff Raether	% diff Robinson
BK	1	1	0	50	160	0.11	0.02	-91.49	1.51	6.67	1.86	11.10	3.09	8.24	2.43	0.73	0.33	0.12	0.05	-91.49	1.51	1.76E-24	4.53E-26	-0.74	0.01	172	29.3	292	-	-	-40.93%	-	-
BK	2	1	0	110	160	-	-	-	-	-	-	-	-	-	-	-	-	-															
BK	3	1	0	110	160	-	-	-	-	-	-	-	-	-	-	-	-	-															
BK	1	1	1	50	160	0.08	0.02	-106.42	2.53	8.26	3.37	13.75	5.61	7.74	3.34	0.62	0.47	0.24	0.08	0.04	-108.98	2.70	1.76E-24	4.53E-26	-0.88	0.02	207	32.5	292	-	-	-29.04%	-	-
BK	2	1	1	110	160	0.05	0.04	-111.80	4.47	3.99	6.45	6.65	10.74	16.82	27.86	0.19																	
BK	3	1	1	110	160	0.10	0.18	-108.70	18.98	5.90	14.03	9.83	23.36	11.06	28.23	0.58																	
BK	1	2	2	50	160	0.95	0.02	-135.60	0.08	4.42	0.11	7.35	0.18	18.44	0.47	4.22	4.93	0.62	0.10	0.10	-136.15	0.57	1.76E-24	4.53E-26	-1.10	0.00	261	29.5	292	-	-	-10.56%	-	-
BK	2	1	2	110	160	0.91	0.03	-136.73	0.16	5.84	0.23	9.72	0.38	14.07	0.57	5.33																	
BK	3	1	2	110	160	0.97	0.04	-136.11	0.18	5.42	0.26	9.03	0.43	15.08	0.73	5.24																	
BK	1	2	1	75	110	0.93	0.06	-86.77	0.21	4.05	0.21	6.74	0.34	12.87	0.69	3.75	3.54	0.19	0.56	0.03	-86.53	0.21	1.76E-24	4.53E-26	-1.40	0.00	334	30.8	319	-	344	4.84%	-	-2.78%
BK	2	2	1	75	110	0.91	0.05	-86.45	0.16	3.81	0.17	6.35	0.28	13.62	0.64	3.47																	
BK	3	2	1	75	110	0.85	0.07	-86.37	0.20	3.98	0.21	6.83	0.35	13.02	0.71	3.39																	
BK	1	2	2	75	110	0.41	0.02	-94.76	0.81	6.09	0.83	10.13	1.38	9.35	1.35	2.48	2.80	0.58	0.44	0.09	-94.31	0.49	1.76E-24	4.53E-26	-1.53	0.01	365	32.7	319	-	344	14.52%	-	6.20%
BK	2	2	2	75	110	0.40	0.02	-94.40	0.63	6.02	0.69	10.02	1.15	9.42	1.14	2.44																	
BK	3	2	2	75	110	0.56	0.03	-93.78	0.66	6.25	0.62	10.41	1.02	9.01	0.95	3.47																	
AT1	1	1	1	140	180	1.02	0.02	-152.18	0.07	4.41	0.09	7.34	0.15	20.72	0.44	4.49	4.68	0.47	1.00	0.10	-151.79	0.51	2.15387E-24	4.55E-26	-1.23	0.00	292	30.0	-	-	-	-	-	-
AT1	2	1	1	140	180	0.91	0.03	-151.98	0.15	4.77	0.21	7.95	0.35	19.12	0.86	4.33																	
AT1	3	1	1	140	180	0.99	0.02	-151.22	0.11	5.25	0.15	8.74	0.25	17.31	0.51	5.21																	
AT1	1	2	1	75	115	0.67	0.07	-93.54	0.12	3.92	0.25	6.53	0.41	14.31	0.92	2.63	2.14	0.49	0.39	0.09	-94.42	1.05	2.16E-24	4.55E-26	-1.53	0.02	365	34.8	-	384	-	-	-4.98%	-
AT1	2	2	1	75	115	0.58	0.15	-95.59	0.22	3.62	0.48	6.03	0.79	15.86	2.13	2.12																	
AT1	3	2	1	75	115	0.43	0.30	-94.13	0.43	3.87	1.07	6.44	1.77	14.61	4.09	1.66																	
AT1	1	2	2	75	115	0.39	0.06	-97.40	0.72	7.30	0.35	12.15	0.59	8.02	0.45	2.87	3.35	0.55	0.61	0.10	-98.13	0.83	2.16E-24	4.55E-26	-1.59	0.01	380	34.3	-	384	-	-	-1.15%	-
AT1	2	2	2	75	115	0.50	0.11	-99.04	1.00	6.40	0.46	10.66	0.76	9.29	0.75	3.23																	
AT1	3	2	2	75	115	0.63	0.20	-97.94	1.63	6.28	0.71	10.45	1.18	9.37	1.21	3.96																	
AT1	1	3	1	75	115	0.83	0.05	-83.33	0.19	4.32	0.27	7.20	0.46	11.57	0.76	3.60	3.59	0.22	1.00	0.06	-82.65	0.61	2.16E-24	4.55E-26	-2.01	0.01	482	37.0	-	473	474	-	1.89%	1.67%
AT1	2	3	1	75	95	0.72	0.07	-82.43	0.41	5.30	0.61	8.83	1.01	9.34	1.11	3.80																	
AT1	3	3	1	75	95	0.79	0.07	-82.17	0.32	4.25	0.46	7.07	0.77	11.62	1.31	3.37																	
AT2	1	1	1	120	160	1.00	0.02	-134.44	0.09	3.86	0.12	6.42	0.21	20.94	0.69	3.84	4.09	0.22	0.93	0.05	-134.50	0.10	1.74E-24	4.53E-26	-1.09	0.00	258	28.5	286	-	-	-9.82%	-	-
AT2	2	1	1	120	160	0.98	0.03	-134.43	0.11	4.28	0.13	7.13	0.22	18.85	0.60	4.19																	
AT2	3	1	1	120	160	1.01	0.01	-134.62	0.06	4.20	0.09	7.00	0.14	19.24	0.40	4.25																	
AT2	1	1	2	120	160	0.06	0.02	-144.28	1.85	5.19	2.75	8.64	4.58	16.70	9.06	0.30	0.30	0.08	0.07	0.02	-144.61	0.29	1.74E-24	4.53E-26	-1.17	0.00	278	29.3	286	-	-	-2.80%	-	-
AT2	2	1	2	120	160	0.06	0.01	-144.76	2.94	6.96	3.85	11.59	6.41	12.49	7.16	0.39																	
AT2	3	1	2	120	160	0.05	0.01	-144.80	1.32	4.62	1.97	7.70	3.28	18.81	8.19	0.22																	
AT2	1	2	1	80	120	0.66	0.18	-88.17	0.19	3.31	0.51	5.51	0.85	16.00	2.51	2.20	2.45	0.23	0.43	0.04	-88.02	0.24	1.74E-24	4.53E-26	-1.43	0.00	340	31.1	318	355	335	7.05%	-4.11%	1.62%
AT2	2	2	1	80	120	0.73	0.20	-88.16	0.16	3.39	0.45	5.65	0.74	15.61	2.08	2.48																	
AT2	3	2	1	80	120	0.75	0.15	-87.74	0.14	3.55	0.36	5.91	0.60	14.85	1.53	2.66																	
AT2	1	2	2	80	120	0.62	0.07	-93.74	1.25	6.51	0.96	10.84	1.60	8.64	1.39	4.01	3.26	0.66	0.57	0.12	-93.41	0.30	1.74E-24	4.53E-26	-1.52	0.00	362	31.8	318	355	335	13.78%	1.92%	8.01%
AT2	2	2	2	80	120	0.45	0.09	-93.16	1.78	6.18	1.19	10.29	1.98	9.05	1.91	2.76																	
AT2	3	2	2	80	120	0.46	0.06	-93.34	1.43	6.58	1.03	10.95	1.72	8.53	1.47	3.01																	
UB	1	5	1	80	160	0.87	0.04	-142.94	0.34	10.18	0.49	16.94	0.82	8.44	0.43	8.83	8.18	1.26	1.00	0.15	-142.60	0.33	1.42E-23	4.63E-26	-5.72	0.01	1390	57.3	-	-	-	-	-	-
UB	2	5	1	80	160	0.76	0.04	-142.28	0.41	8.90	0.58	14.82	0.96	9.60	0.65	6.72																	
UB	3	5	1	80	160	0.96	0.04	-142.57	0.33	9.39	0.47	15.64	0.78	9.12	0.47	8.98																	
UB	1	6	1	80	160	0.95	0.02	-138.34	0.11	6.09	0.16	10.15	0.26	13.63	0.36	5.78	5.98	0.19	1.00	0.03	-137.76	0.52	1.42E-23	4.63E-26	-6.63	0.03	1613	65.3	-	-	-	-	-	-
UB	2	6	1	80	160	0.99	0.03	-137.31	0.13	6.23	0.18	10.37	0.31	13.24	0.40	6.16																	
UB	3	6	1	80	160	0.95	0.02	-137.63	0.12	6.30	0.17	10.48	0.28	13.13	0.37	6.00																	
UB	1	7	1	80	160	0.93	0.04	-134.49	0.19	5.70	0.27	9.48	0.44	14.18	0.68	5.30	5.14	0.20	1.00	0.04	-133.94	0.52	1.42E-23	4.63E-26	-7.52	0.03	1831	71.2	-	-	1910	-	-	-4.13%
UB	2	7	1	80	160	0.96	0.03	-133.88	0.12	5.41	0.17	9.01	0.29	14.85	0.49	5.20																	
UB	3	7	1	80	160	0.96	0.04	-133.46	0.17	5.14	0.25	8.56	0.41	15.60	0.77	4.92																	
UB	1	8	1	80	160	0.85	0.04	-132.18	0.15	4.29	0.21	7.15	0.36	18.50	0.94	3.66	3.97	0.34	1.00	0.09	-131.43	0.68	1.42E-23	4.63E-26	-8.43	0.04	2055	79.8	-	-	1990	-	-	3.25%
UB	2	8	1	80	160	1.01	0.05	-130.88	0.18	4.30	0.25	7.16	0.41	18.27	1.08	4.33																	
UB	3	8	1	80	160	0.76	0.06	-131.22	0.32	5.17	0.45	8.62	0.75	15.23	1.36	3.91																	

Supplementary Table 10: Peptides: detailed results at $T_{ESI} = 400$ K.

Species	Trial	Charge	Peak	Start	End [V]	a	∂ 95%CI	b	∂ 95%CI	c	∂ 95%CI	FWHM	E(FWHM)	R	E(F)	d	avg d	E(d)	Fraction	Efficiency	avg c [V]	c diag.	Ion Mass [kg]	Red. Mass [kg]	β x10^6	Eβ β x10^6	Ω [Å²]	E(Ω)	Hill1999	Paethner2009	Robinson2010	%diff Hill	%diff Paethner	%diff Robinson
BK	1	1	75	175	0.02	0.01	-112.43	2.35	3.26	15.42	5.53	7.29	2.79	0.15	0.14	0.01	0.02	0.00	-113.45	1.00	1.78E-24	4.53E-26	-0.92	0.01	216	25.3	232	-	-	-25.35%	-	-
BK	2	1	75	175	0.02	0.01	-113.43	2.09	7.87	2.96	13.10	4.95	8.67	3.44	0.13																		
BK	3	1	75	175	0.02	0.01	-114.43	2.49	9.01	3.61	15.00	6.01	7.63	3.22	0.14																		
BK	1	2	75	175	1.00	0.02	-135.67	0.11	4.06	0.09	6.75	0.15	20.03	0.46	4.06	0.16	4.07	0.16	0.62	0.02	-135.69	0.20	1.78E-24	4.53E-26	-1.10	0.00	260	27.9	232	-	-	-10.86%	-	-
BK	2	2	75	175	0.99	0.01	-135.68	0.08	4.27	0.06	7.11	0.14	19.10	0.38	4.23																		
BK	3	2	75	175	0.97	0.02	-135.50	0.09	4.02	0.06	6.69	0.13	20.26	0.42	3.92																		
BK	1	3	75	175	0.31	0.02	-143.71	0.39	4.94	0.95	8.22	1.58	17.48	3.41	1.51	1.40	1.51	0.14	0.21	0.02	-143.97	0.37	1.78E-24	4.53E-26	-1.17	0.00	277	28.0	232	-	-	-5.25%	-	-
BK	2	3	75	175	0.30	0.04	-143.90	0.27	4.16	0.52	6.93	0.86	20.76	2.63	1.24																		
BK	3	3	75	175	0.27	0.01	-144.39	0.35	5.45	1.03	9.07	1.81	15.91	3.22	1.46																		
BK	1	4	75	175	0.14	0.02	-152.73	1.22	5.40	1.58	8.99	2.63	17.00	5.12	0.75	0.77	0.22	0.12	0.12	0.03	-152.72	0.38	1.78E-24	4.53E-26	-1.24	0.00	294	28.3	232	-	-	0.70%	-	-
BK	2	4	75	175	0.14	0.01	-152.35	1.21	6.86	1.94	11.42	3.23	13.34	3.88	0.99																		
BK	3	4	75	175	0.13	0.03	-153.10	0.76	4.22	1.01	7.03	1.69	21.79	5.33	0.56																		
BK	1	5	75	175	0.03	0.01	-165.61	2.05	6.32	2.93	10.53	4.88	15.73	7.46	0.19	0.22	0.08	0.03	0.03	0.01	-165.29	1.77	1.78E-24	4.53E-26	-1.34	0.01	319	26.1	232	-	-	9.25%	-	-
BK	2	5	75	175	0.03	0.01	-166.88	2.47	6.04	3.41	10.05	5.68	16.60	9.63	0.16																		
BK	3	5	75	175	0.04	0.01	-163.36	2.63	7.83	3.32	13.05	5.52	12.52	5.51	0.30																		
BK	1	2	1	175	0.66	0.58	-93.19	0.93	5.37	1.32	3.94	2.20	8.97	2.07	3.96	2.92	1.14	0.35	0.35	0.14	-88.73	0.41	1.78E-24	4.53E-26	-1.44	0.01	343	28.6	319	-	344	7.58%	-	-0.24%
BK	2	2	1	175	0.47	0.11	-88.45	0.24	3.62	0.63	6.03	1.04	14.66	2.57	1.71																		
BK	3	2	1	175	0.61	0.26	-88.55	0.35	5.08	0.61	8.47	1.35	10.46	1.70	3.08																		
BK	1	2	2	175	0.50	0.33	-95.84	5.92	8.71	3.01	14.50	5.02	6.61	2.70	4.33	5.39	1.24	0.65	0.65	0.15	-95.37	0.43	1.78E-24	4.53E-26	-1.55	0.01	370	29.1	319	-	344	15.84%	-	7.42%
BK	2	2	2	175	0.63	0.04	-94.99	0.71	8.15	0.56	13.58	0.94	7.00	0.54	6.75																		
BK	3	2	2	175	0.61	0.13	-95.27	2.26	8.39	1.36	13.96	2.27	6.82	1.27	5.08																		
ATI	1	1	1	70	200	0.01	0.00	-126.24	5.01	13.29	7.32	22.12	12.19	5.71	3.37	0.10	0.07	0.03	0.01	0.01	-127.32	3.84	2.15E-24	4.55E-26	-1.03	0.03	243	20.3	-	-	-	-	-	-
ATI	2	1	1	70	200	0.01	0.01	-131.58	4.45	7.16	6.30	11.93	10.50	11.03	10.08	0.06																		
ATI	3	1	1	70	200	0.01	0.01	-124.13	6.85	7.39	9.68	12.30	16.13	10.09	13.79	0.04																		
ATI	1	2	1	70	200	0.02	0.01	-153.31	0.02	4.46	0.03	7.42	0.05	20.66	0.15	4.54	4.54	0.03	0.74	0.00	-153.25	0.15	2.15E-24	4.55E-26	-1.24	0.00	294	28.8	-	-	-	-	-	-
ATI	2	2	1	70	200	0.02	0.01	-153.37	0.03	4.49	0.04	7.46	0.07	20.50	0.19	4.57																		
ATI	3	2	1	70	200	0.01	0.01	-153.08	0.03	4.47	0.04	7.44	0.07	20.57	0.20	4.51																		
ATI	1	3	1	70	200	0.15	0.01	-183.73	0.44	6.00	0.52	9.98	0.87	17.00	1.53	0.90	0.65	0.04	0.14	0.01	-183.20	0.53	2.15E-24	4.55E-26	-1.37	0.00	326	28.8	-	-	-	-	-	-
ATI	2	3	1	70	200	0.14	0.01	-186.88	0.52	5.81	0.65	9.67	1.07	17.44	1.99	0.82																		
ATI	3	3	1	70	200	0.16	0.01	-183.19	0.48	5.23	0.54	8.72	0.91	19.41	2.07	0.83																		
ATI	1	4	1	70	200	0.11	0.01	-180.46	0.57	5.60	0.62	9.33	1.04	19.35	2.21	0.62	0.67	0.08	0.11	0.01	-180.07	0.35	2.15E-24	4.55E-26	-1.46	0.00	348	29.6	-	-	-	-	-	-
ATI	2	4	1	70	200	0.10	0.01	-173.96	0.77	6.12	0.89	10.19	1.46	17.67	2.64	0.62																		
ATI	3	4	1	70	200	0.12	0.01	-173.79	0.71	6.17	0.84	10.28	1.39	17.50	2.44	0.76																		
ATI	1	2	2	70	200	0.46	0.08	-95.31	0.17	2.83	0.42	4.72	0.70	20.19	3.04	1.37	1.96	1.18	0.21	0.13	-95.37	0.06	2.16E-24	4.55E-26	-1.54	0.00	369	30.5	-	384	-	-4.00%	-	-
ATI	2	2	2	70	200	0.67	0.21	-95.37	1.02	3.82	0.64	6.36	0.96	15.00	2.67	3.32																		
ATI	3	2	2	70	200	0.53	0.12	-95.42	0.25	2.24	0.51	3.74	0.85	25.54	5.90	1.18																		
ATI	1	2	2	70	200	0.68	0.02	-102.15	0.42	7.56	0.52	12.59	0.86	8.11	0.53	6.62	4.72	2.21	0.52	0.24	-101.32	0.75	2.16E-24	4.55E-26	-1.64	0.01	392	28.3	-	384	-	2.14%	-	-
ATI	2	2	2	70	200	0.64	0.37	-100.69	0.69	3.58	1.60	5.95	2.67	16.91	7.73	2.30																		
ATI	3	2	2	70	200	0.63	0.07	-101.13	1.15	6.35	1.26	10.57	2.11	9.57	2.02	5.25	2.21	0.53	0.24	0.06	-109.31	3.02	2.16E-24	4.55E-26	-1.77	0.05	424	20.1	-	384	-	10.38%	-	-
ATI	1	3	2	70	200	-	-	-	-	-	-	-	-	12.97	5.28	2.59																		
ATI	2	3	2	70	200	0.52	0.09	-107.18	1.73	4.96	1.93	8.26	3.21	11.73	6.28	1.64																		
ATI	3	3	2	70	200	0.32	0.09	-111.44	2.10	5.68	2.51	9.45	4.84	11.73	6.28	1.64																		
ATI	1	2	4	70	200	0.08	0.03	-120.74	1.81	4.51	2.65	7.51	4.41	16.07	9.88	0.38	0.28	0.09	0.03	0.01	-119.67	2.45	2.16E-24	4.55E-26	-1.94	0.04	465	23.3	-	384	-	21.07%	-	-
ATI	2	2	4	70	200	0.08	0.03	-116.87	1.84	3.33	2.22	5.54	3.69	21.09	14.37	0.25																		
ATI	3	2	4	70	200	0.06	0.05	-121.41	3.27	3.30	4.23	5.50	7.04	22.07	28.63	0.20																		
ATI	1	3	1	70	200	-	-	-	-	-	-	-	-	8.56	1.46	3.32	3.77	0.64	1.00	0.17	-97.41	0.39	2.16E-24	4.55E-26	-2.12	0.01	510	31.7	-	473	474	-	7.88%	7.65%
ATI	2	3	1	70	200	0.54	0.08	-97.14	0.70	6.11	0.99	10.18	1.66	7.84	1.61	4.22																		
ATI	3	3	1	70	200	0.63	0.11	-97.69	0.93	6.71	1.31	11.18	2.18	7.84	1.61	4.22	0.14	0.06	0.02	0.01	-115.88	0.76	1.74E-24	4.53E-26	-0.94	0.01	221	25.9	286	-	-	-22.74%	-	-
AT12	1	1	1	75	180	0.02	0.01	-115.83	3.33	10.75	6.01	17.90	10.01	6.47	3.84	0.17	0.14	0.06	0.02	0.01	-115.88	0.76	1.74E-24	4.53E-26	-0.94	0.01	221	25.9	286	-	-	-22.74%	-	-
AT12	2	1	1	75	180	0.01	0.01	-115.15	5.41	7.66	7.76	13.09	12.32	8.60	9.03	0.08																		
AT12	3	1	1	75	180	0.02	0.01	-116.66	3.29	9.96	5.00	16.53	8.33	7.03	3.73	0.18																		
AT12	1	2	1	75	180	0.36	0.04	-135.72	0.04	4.18	0.06	6.96	0.11	19.51	0.31	4.11	4.25	0.15	0.49	0.02	-135.76	0.15	1.74E-24	4.53E-26	-1.10	0.00	260	28.0	286	-	-	-8.94%	-	-
AT12	2	2	1	75	180	1.01	0.01	-135.64	0.04	4.36	0.06	7.25	0.10	18.70	0.27	4.41																		
AT12	3	2	1	75	180	1.01	0.01	-135.93	0.04	4.19	0.06	6.98	0.10	19.48	0.28	4.21																		
AT12	1	3	1	75	180	0.26	0.01	-150.02	0.51	6.19	0.67	10.31	1.11	14.55	1.62	1.53	1.88	0.67	0.22	0.08	-150.05	0.18	1.74E-24	4.53E-26	-1.22	0.00	289	28.6	286	-	-	0.98%	-	-
AT12	2	3	1	75	180	0.47	0.01	-150.24	0.23	5.68	0.30	9.46	0.51	15.89	0.67	2.64																		
AT12	3	3	1	75	180	0.30	0.01	-149.89	0.30	4.75	0.36	7.91	0.59	18.95	1.46	1.41																		
AT12	1	4	1	75	180	0.37	0.02	-180.06	0.31	5.03	0.31	8.38	0.51	19.10	1.20	1.65	2.47	0.58	0.28	0.07	-159.98	0.39	1.74E-24	4.53E-26	-1.30	0.00	309	28.6	286	-	-	7.88%	-	-
AT12	2	4	1	75	180	0.60	0.01	-180.34	0.17	5.00	0.19	8.32	0.31	19.27	0.73	2.58																		
AT12	3	4	1	75	180	0.46	0.01	-153.56	0.20	5.40	0.25	8.99	0.41	17.76	0.83	2.58																		
AT12	1	2	2	75	180	0.72	0.42	-91.71	0.98	5.67	1.56	9.45	2.80	9.71	2.78	4.08	4.53	0.63	0.63	0.09	-93.36	2.32	1.74E-24	4.53E-26	-1.51	0.04	362	21.4	318	355	335	13.71%	1.86%	7.94%
AT12	2	2	2	75	180	-	-	-	-	-	-	-	-	8.86	2.02	4.98																		
AT12	3	2	2	75	180	0.77	0.08	-95.00	0.99	6.44	1.40	10.72	2.34	8.86	2.02	4.98																		
AT12	1	2	2	75	180	0.40	0.15	-101.21	6.37	9.85	5.52	16.40	9.20	6.17	3.89	3.98	2.64	1.89	0.37	0.26	-102.11	1.27	1.74E-24	4.53E-26	-1.66	0.02	396	26.4	318	355	335	24.64%	11.65%	18.31%
AT12	2	2	2	75	180	-	-	-	-	-	-	-	-	-	-	-																		
AT12	3	2	2	75	180	0.51	0.18	-103.00	0.64	2.58	1.05	4.29	1.74	23.99	9.90	1.31																		

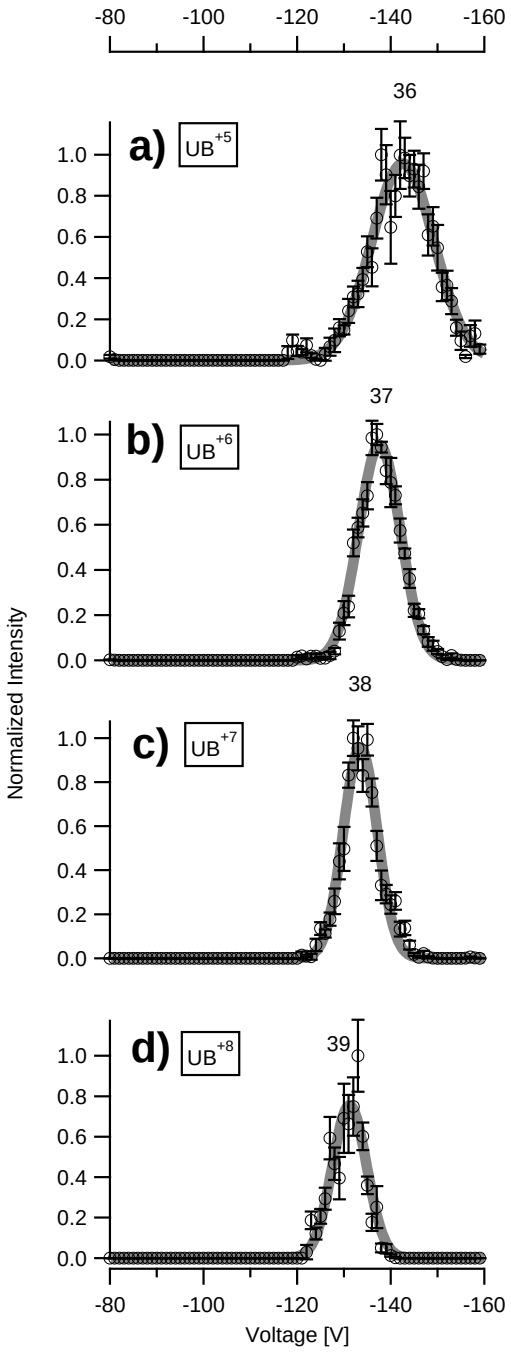

Supplementary Figure 5: A single experimental classification of UB, showing mass–resolved, normalized signal as a function of ϕ. Error bars on the circular markers indicate 1 standard deviation of the normalized signal at that ϕ for that one scan. Each resolvable Gaussian peak is labeled with a unique identifier number. The thick gray line is the Gaussian–fitted function to the signal. a) UB^{+5} at $T_{ESI} = 298$ K. b) UB^{+6} at $T_{ESI} = 298$ K. c) UB^{+7} at $T_{ESI} = 298$ K. d) UB^{+8} at $T_{ESI} = 298$ K.

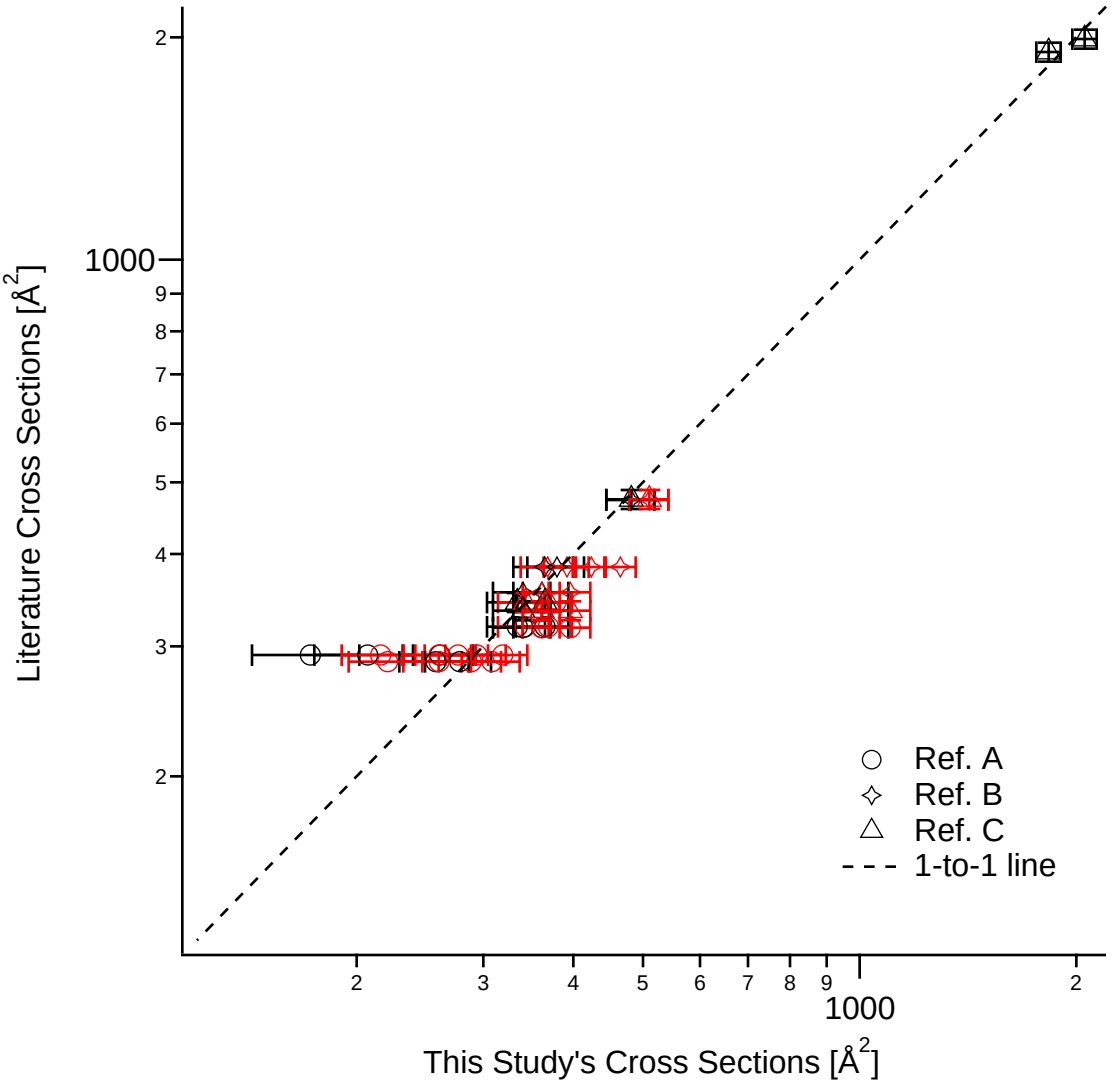

Supplementary Figure 6: Measured cross sections values in this study against those from other studies. Black markers indicate $T_{ESI} = 298$ K and red markers indicate $T_{ESI} = 400$ K. Horizontal error bars denote 1 standard deviation of triplicates. Vertical error bars indicate that study's estimated error, if provided. Ref. A: [9]. Ref. B: [20]. Ref. C: [8].

Supplementary Table 11: Model peptides: detailed results at $T_{ESI} = 298$ K.

Sequence	TEMPO	CID	charge	*m/z*	Start ϕ [V]	End ϕ [V]	*a*	*a* 95%CI	*b*	*b* 95%CI	*c*	*c* 95%CI	FWHM	E(FWHM)	*R*	E(*R*)	Ion Mass [kg]	Red. Mass [kg]	θx10^{16}	E(θ)x10^{16}	Ω [Å^2]	E(Ω)
AA_AAA_AA	no	no	1	969.5-974	100	120	0.92	0.04	-110.20	0.15	3.97	0.21	6.62	0.35	16.65	0.90	1.61E-24	4.52E-26	-0.89	0.001	210	26.9
AARAAATAA	no	yes	1	281.5-283.7	100	120	0.90	0.06	-111.65	0.23	4.10	0.32	6.83	0.54	16.34	1.32	4.69E-25	4.23E-26	-0.94	0.002	220	26.9
AARAAATAA	no	yes	1	352.5-355	100	120	0.87	0.07	-112.01	0.21	3.48	0.30	5.79	0.51	19.35	1.73	5.87E-25	4.31E-26	-0.93	0.002	219	26.9
AARAAATAA	no	yes	1	423.5-425.7	100	120	0.94	0.08	-111.12	0.22	3.21	0.31	5.34	0.51	20.81	2.02	7.05E-25	4.36E-26	-0.92	0.002	216	26.9
AATAAARAA	no	yes	1	367.5-369.5	100	120	0.82	0.09	-112.07	0.35	4.01	0.49	6.68	0.82	16.78	2.11	6.12E-25	4.32E-26	-0.93	0.003	219	26.7
AATAAARAA	no	yes	1	438.5-440.7	100	120	0.89	0.07	-111.90	0.24	3.68	0.34	6.12	0.57	18.27	1.74	7.30E-25	4.37E-26	-0.92	0.002	217	26.8
AATAAARAA	no	yes	1	529.6-531.8	100	120	0.84	0.07	-112.18	0.26	3.57	0.36	5.94	0.60	18.87	1.96	8.81E-25	4.42E-26	-0.92	0.002	216	26.8
AARAAATAA	yes	yes	1	526-529	120	150	0.96	0.02	-128.48	0.07	3.81	0.10	6.35	0.17	20.23	0.56	8.76E-25	4.42E-26	-1.06	0.001	249	27.9
AARAAATAA	yes	yes	1	570-575	120	150	0.96	0.03	-128.63	0.10	4.00	0.15	6.67	0.24	19.30	0.72	9.50E-25	4.43E-26	-1.05	0.001	249	27.8
AATAAARAA	yes	yes	1	529.8-534	120	150	0.97	0.02	-135.66	0.09	4.20	0.12	7.00	0.20	19.39	0.58	8.83E-25	4.42E-26	-1.11	0.001	264	28.2
AATAAARAA	yes	yes	1	613-617	120	150	0.98	0.02	-135.72	0.07	4.19	0.11	6.98	0.18	19.45	0.50	1.02E-24	4.45E-26	-1.11	0.001	263	28.2
AARAA_A_A	no	no	1	868-873	115	135	0.97	0.02	-120.34	0.07	3.42	0.10	5.69	0.17	21.13	0.65	1.45E-24	4.50E-26	-0.98	0.001	230	27.5
AARAAHAMA	no	yes	1	631.5-635	110	130	0.91	0.05	-119.66	0.16	3.80	0.23	6.32	0.38	18.93	1.17	1.05E-24	4.45E-26	-0.98	0.001	230	27.3
AARAAMAHA	no	yes	1	642.5-646	110	130	0.89	0.06	-120.96	0.20	3.75	0.29	6.24	0.48	19.37	1.53	1.07E-24	4.46E-26	-0.99	0.002	233	27.3
AARAA_A_A	yes	no	1	1065.5-1070	130	160	0.87	0.05	-141.97	0.21	4.72	0.30	7.85	0.50	18.08	1.18	1.77E-24	4.53E-26	-1.15	0.002	273	28.2
AARAAHAMA	yes	yes	1	591.5-594	130	160	0.94	0.05	-140.28	0.18	4.05	0.25	6.75	0.42	20.78	1.31	9.84E-25	4.44E-26	-1.15	0.001	272	28.2
AARAAMAHA	yes	yes	1	793.8-795.9	130	160	0.95	0.04	-143.05	0.14	3.73	0.20	6.22	0.33	23.00	1.23	1.32E-24	4.49E-26	-1.17	0.001	276	28.4

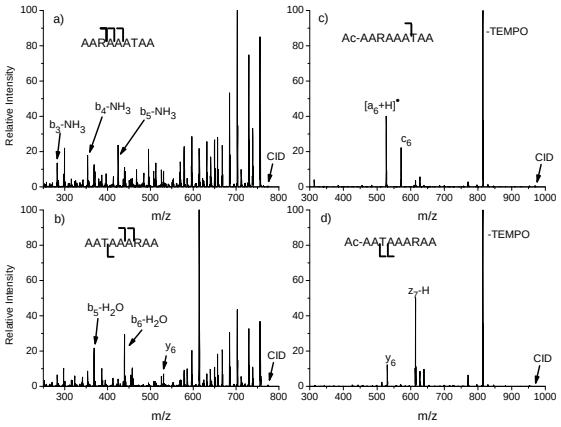

Supplementary Figure 7: CID spectra of the peptide isomers a) AARAAATAA and b) AATAAARAA. Corresponding FRIPS spectra are shown in c) and d). Labeled peaks are product ions specific to each isomer used for identification during separation by the ROMIAC; other peaks common to both isomers are not labeled for clarity. Product ions in the FRIPS spectrum are referenced to the acetyl radical generated by loss of the TEMPO moiety.

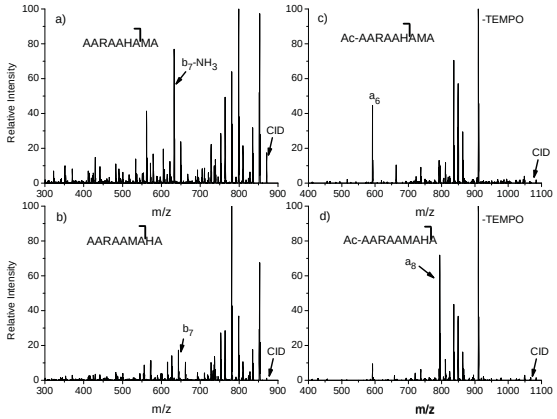

Supplementary Figure 8: Same as Fig. S7, but for a) AARAAHAMA and b) AARAAMAHA. orresponding FRIPS spectra are shown in c) and d).

References

[1] R. Hodyss, H.A. Cox, and J.L. Beauchamp. Bioconjugates for tunable peptide fragmentation: free radical initiated peptide sequencing (FRIPS). *Journal of the American Chemical Society*, 127(36):12436–7, September 2005.

[2] Q. Sun, H. Nelson, T. Ly, B.M. Stoltz, and R.R. Julian. Side chain chemistry mediates backbone fragmentation in hydrogen deficient peptide radicals. *Journal of Proteome Research*, 8:958–966, 2009.

[3] M. Lee, M. Kang, M. Moon, and H.B. Oh. Gas-phase peptide sequencing by TEMPO-mediated radical generation. *Analyst*, 134(8):1706–12, August 2009.

[4] C.H. Sohn. *New reagents and methods for mass spectrometry-based proteomics investigations*. Dissertation (ph.d.), California Institute of Technology, 2011.

[5] R. Fernández-Maestre, C.S. Harden, R.G. Ewing, C.L. Crawford, and H.H. Hill. Chemical standards in ion mobility spectrometry. *The Analyst*, 135(6):1433–42, June 2010.

[6] J. Viidanoja, A. Sysoev, A. Adamov, and T. Kotiaho. Tetraalkylammonium halides as chemical standards for positive electrospray ionization with ion mobility spectrometry/mass spectrometry. *Rapid Communications in Mass Spectrometry*, 19(21):3051–5, January 2005.

[7] G. Kaur-Atwal, G. O Connor, A.A. Aksenov, V. Bocos-Bintintan, C.L. Paul Thomas, and C.S. Creaser. Chemical standards for ion mobility spectrometry: a review. *International Journal for Ion Mobility Spectrometry*, 12(1):1–14, May 2009.

[8] M.F. Bush, Z. Hall, K. Giles, J. Hoyes, C.V. Robinson, and B.T. Ruotolo. Collision cross sections of proteins and their complexes: a calibration framework and database for gas-phase structural biology. *Analytical Chemistry*, 82(22):9557–65, November 2010.

[9] C. Wu, J. Klasmeier, and H.H. Hill. Atmospheric pressure ion mobility spectrometry of protonated and sodiated peptides. *Rapid Communications in Mass Spectrometry*, 13(12):1138–42, January 1999.

[10] H.E. Revercomb and E.A. Mason. Theory of plasma chromatography/gaseous electrophoresis - a review. *Analytical Chemistry*, 47(7):970–983, June 1975.

[11] G.A. Eiceman and Z. Karpas. *Ion mobility spectrometry*. CRC Press, 2010.

[12] T. Wyttenbach, G. von Helden, and M.T. Bowers. Gas-phase conformation of biological molecules: Bradykinin. *Journal of the American Chemical Society*, 118(35):8355–8364, 1996.

[13] A.E. Counterman, S.J. Valentine, C.A. Srebalus, S.C. Henderson, C.S. Hoaglund, and D.E. Clemmer. High-order structure and dissociation of gaseous peptide aggregates that are hidden in mass spectra. *Journal of the American Society for Mass Spectrometry*, 9(8):743–59, August 1998.

[14] A.A. Shvartsburg, F. Li, K. Tang, and R.D. Smith. Characterizing the structures and folding of free proteins using 2-D gas-phase separations: observation of multiple unfolded conformers. *Analytical Chemistry*, 78(10):3304–3315, 2006.

[15] A.A. Shvartsburg, F. Li, K. Tang, and R.D. Smith. High-resolution field asymmetric waveform ion mobility spectrometry using new planar geometry analyzers. *Analytical Chemistry*, 78(11):3706–14, June 2006.

[16] N.A. Pierson, L. Chen, S.J. Valentine, D.H. Russell, and D.E. Clemmer. Number of solution states of bradykinin from ion mobility and mass spectrometry measurements. *Journal of the American Chemical Society*, 133(35):13810–13813, 2011.

[17] T. Wyttenbach and M.T. Bowers. Structural stability from solution to the gas phase: native solution structure of ubiquitin survives analysis in a solvent-free ion mobility-mass spectrometry environment. *The Journal of Physical Chemistry. B*, 115(42):12266–75, October 2011.

[18] C. Wu, W.F. Siems, G.R. Asbury, and H.H. Hill. Electrospray ionization high-resolution ion mobility spectrometry-mass spectrometry. *Analytical Chemistry*, 70(23):4929–4938, 1998.

[19] T. Wyttenbach, C. Bleiholder, and M.T. Bowers. Factors contributing to the collision cross section of polyatomic ions in the kilodalton to gigadalton range: application to ion mobility measurements. *Analytical Chemistry*, page Article ASAP, January 2013.

[20] G. Baykut, O. von Halem, and O. Raether. Applying a dynamic method to the measurement of ion mobility. *Journal of the American Society for Mass Spectrometry*, 20(11):2070–81, November 2009.